Supplemental Information

NRF2 is a major target of ARF in p53-independent tumor suppression

Delin Chen, Omid Tavana, Bo Chu, Luke Erber, Yue Chen,

Richard Baer and Wei Gu

Figure S1.

A

Protein Name	No. of Peptide
ARF	2
CBP	>20
p300	>20
MafG	11
MafK	7
MafF	6
Keap1	17

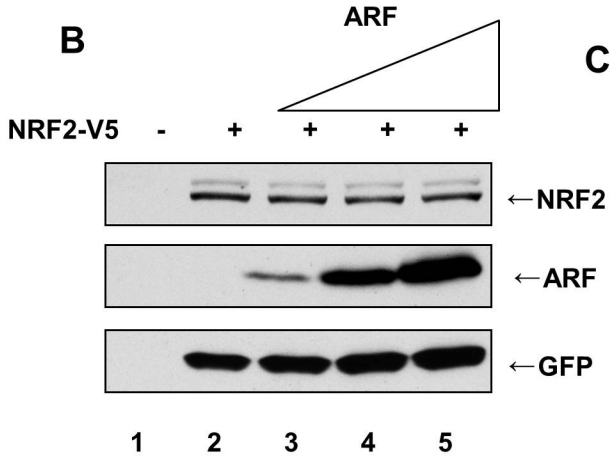

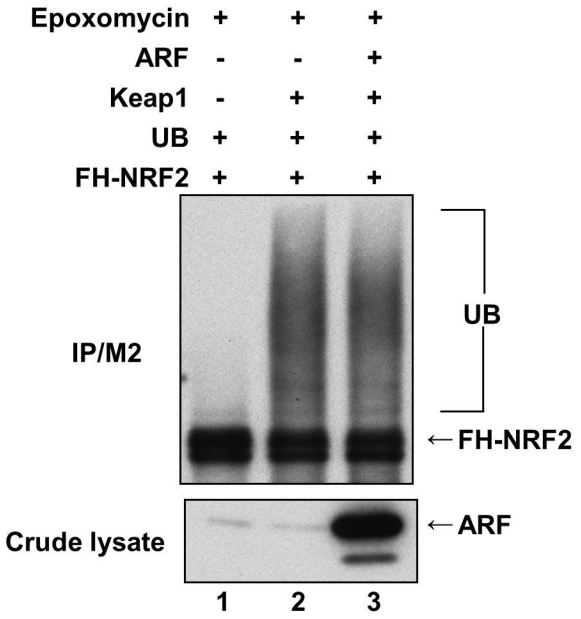

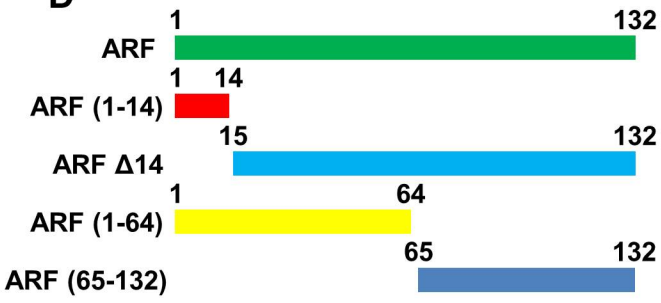

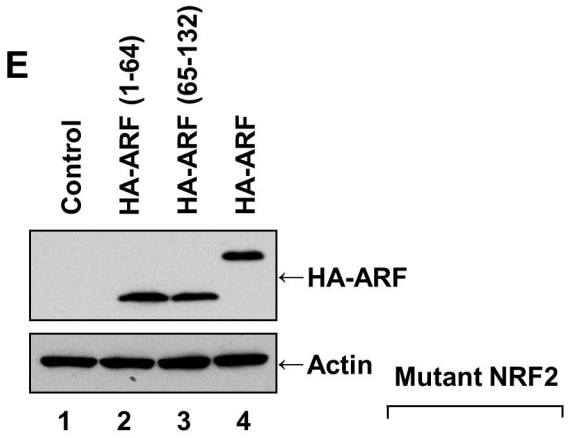

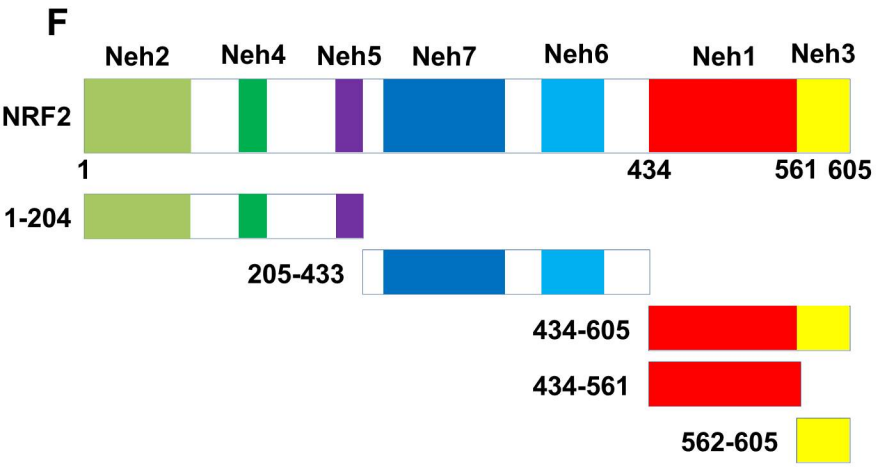

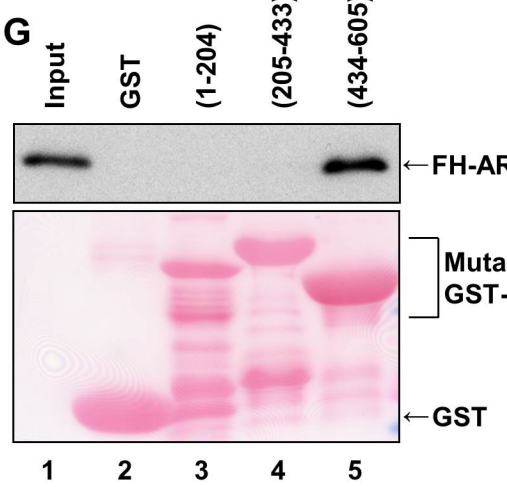

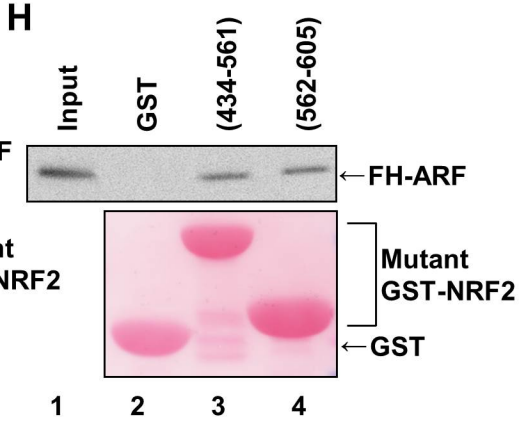

Figure S1. ARF binds with NRF2 protein but does not affect NRF2 ubiquitination or stability, related to Figure 1.

A. The major components of the Flag-HA-NRF2 protein complex (ARF, CBP, p300, MafG, MafK, MafF and Keap1) and the numbers of unique peptides identified by mass spectrometry analysis are shown.
B. Extracts from 293 cells transfected with expression vectors encoding NRF2-V5 and differing amounts of ARF were immunoblotted with antibodies specific for V5, ARF and GFP.
C. ARF did not affect NRF2 ubiquitination mediated by Keap1. 293 cells were transfected with expression vectors encoding FH-NRF2, Ubiquitin, Keap1, and/or ARF as indicated. Cells were treated with proteasome inhibitor for 6 hrs before harvesting. Lysates were immunoprecipitated with FLAG-M2 beads, and the fractionated proteins were immunoblotted with HA antibody (upper panel) or ARF antibody (crude lysates; lower panel).
D. Diagrams of ARF and mutant protein constructs
E. The expressions of HA-ARF (1-64), HA-ARF (65-132) were comparable to full length ARF, related to Figure 1H. Extracts from H1299 cells transfected with expression vectors encoding HA-ARF (1-65), HA-ARF (65-132) or full length HA-ARF were immunoblotted with antibodies for HA (ARF and ARF mutants), and Actin.
F. Diagram of the structure of NRF2 protein and NRF2 mutants
G. Western blot analysis of an *in vitro* GST pull-down assay of highly purified FH-ARF protein incubated with GST-NRF2 (1-204) (lane 3), GST-NRF2 (205-433) (lane 4), GST-NRF2 (434-605) (lane 5) or GST alone (lane 2).
H. Western blot analysis of an *in vitro* GST pull-down assay of highly purified FH-ARF protein incubated with GST-NRF2 (434-561) (lane 3), GST-NRF2 (562-605) (lane 4), or GST alone (lane 2).

Figure S2.

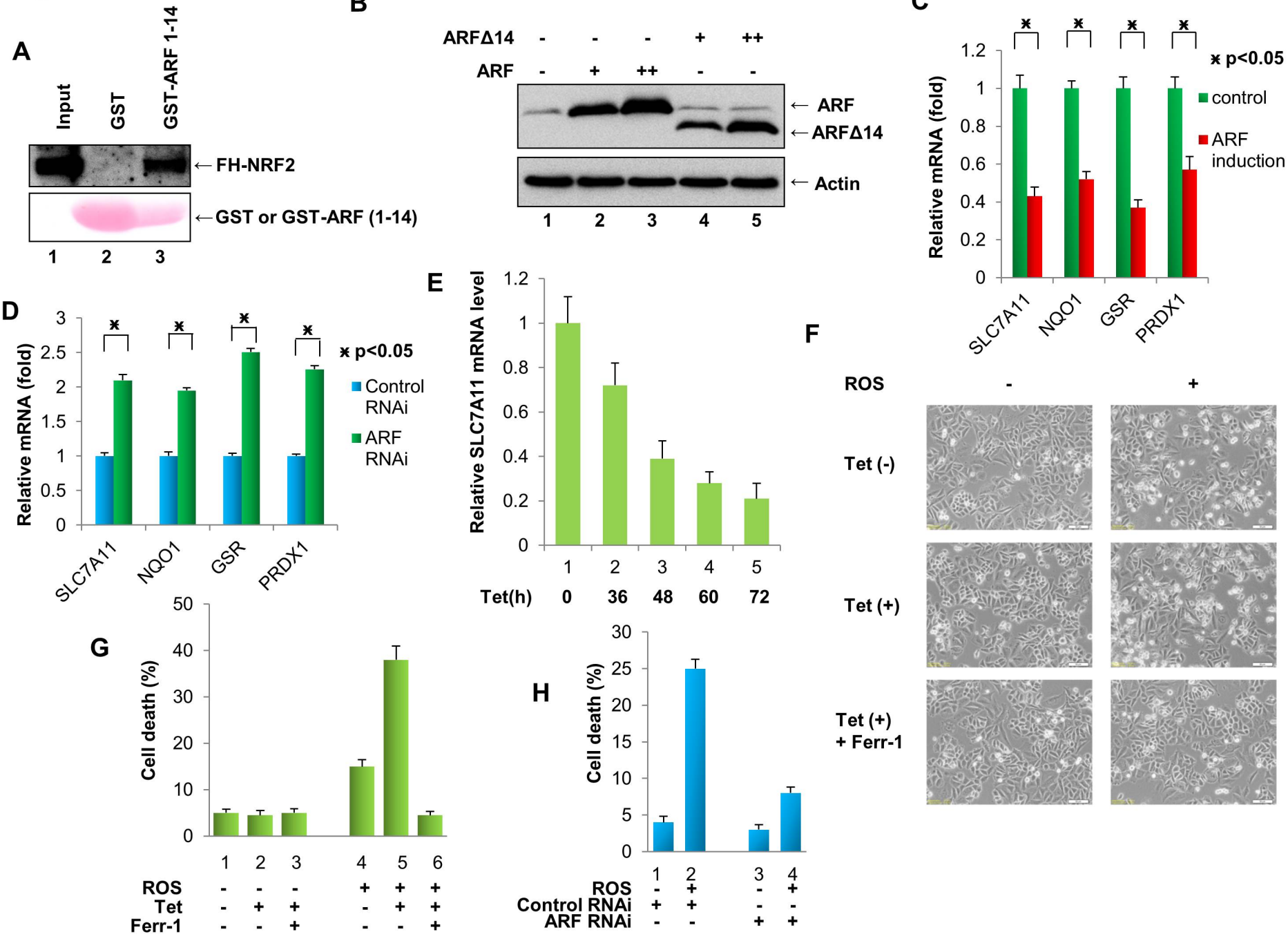
A
Input
GST
GST-ARF 1-14
← FH-NRF2
← GST or GST-ARF (1-14)
1 2 3
B
ARFΔ14 - - - + ++
ARF - + ++ - -
← ARF
← ARFΔ14
← Actin
1 2 3 4 5
C
Relative mRNA (fold)
* p<0.05
control
ARF induction
SLC7A11
NQO1
GSR
PRDX1
D
Relative mRNA (fold)
* p<0.05
Control RNAi
ARF RNAi
SLC7A11
NQO1
GSR
PRDX1
E
Relative SLC7A11 mRNA level
1 2 3 4 5
Tet(h) 0 36 48 60 72
F
ROS - +
Tet (-)
Tet (+)
Tet (+) + Ferr-1
G
Cell death (%)
1 2 3 4 5 6
ROS - - - + + +
Tet - + + - + +
Ferr-1 - - + - - +
H
Cell death (%)
1 2 3 4
ROS - + - +
Control RNAi + + - -
ARF RNAi - - + +

Figure S2. ARF negatively regulates NRF2 function, related to Figure 2.

A. Western blot analysis of an *in vitro* GST pull-down assay of highly purified FH-NRF2 protein incubated with GST-ARF (1-14) (lane 3), or GST alone (lane 2).
B. The protein expressions of ARF as well as ARFΔ14. Extracts from H1299 cells transfected with same expression vectors as in the Figure 2B were immunoblotted with antibodies for ARF and Actin.
C. qPCR analysis of mRNAs levels of NRF2 transcriptional targets (SLC7A11, NQO1, GSR, and PRDX1) in ARF-inducible SaoS2 cells (Tet-on) cultured in the presence or absence of doxycycline (error bars, s. d.; n=3).
D. qPCR analysis of the mRNAs levels of NRF2 targets (SLC7a11, NQO1, GSR and PRDX1) in native SaoS2 cells treated with an ARF-specific or control RNAi (error bars, s. d.; n=3).
E. qPCR analysis of mRNAs levels of NRF2 transcriptional target (SLC7A11) in ARF-inducible H1299 cells cultured in the presence (Tet-on) of doxycycline at different time points as shown in Figure 2E (error bars, s.d ; n=3).
F. Representative phase-contrast images of ROS-treated ARF-inducible SaoS2 cells (Tet-on) cultured with or without doxycycline and/or Ferrostatin-1 (Ferr-1) as indicated.
G. Quantification of ROS-mediated cell death from the samples shown in panel S2F (error bars, s.d from three technical replicates).
H. Quantification of ROS-mediated cell death from the SaoS2 cells after an ARF-specific or control RNAi knock down. (error bars, s.d from three technical replicates).

Figure S3.

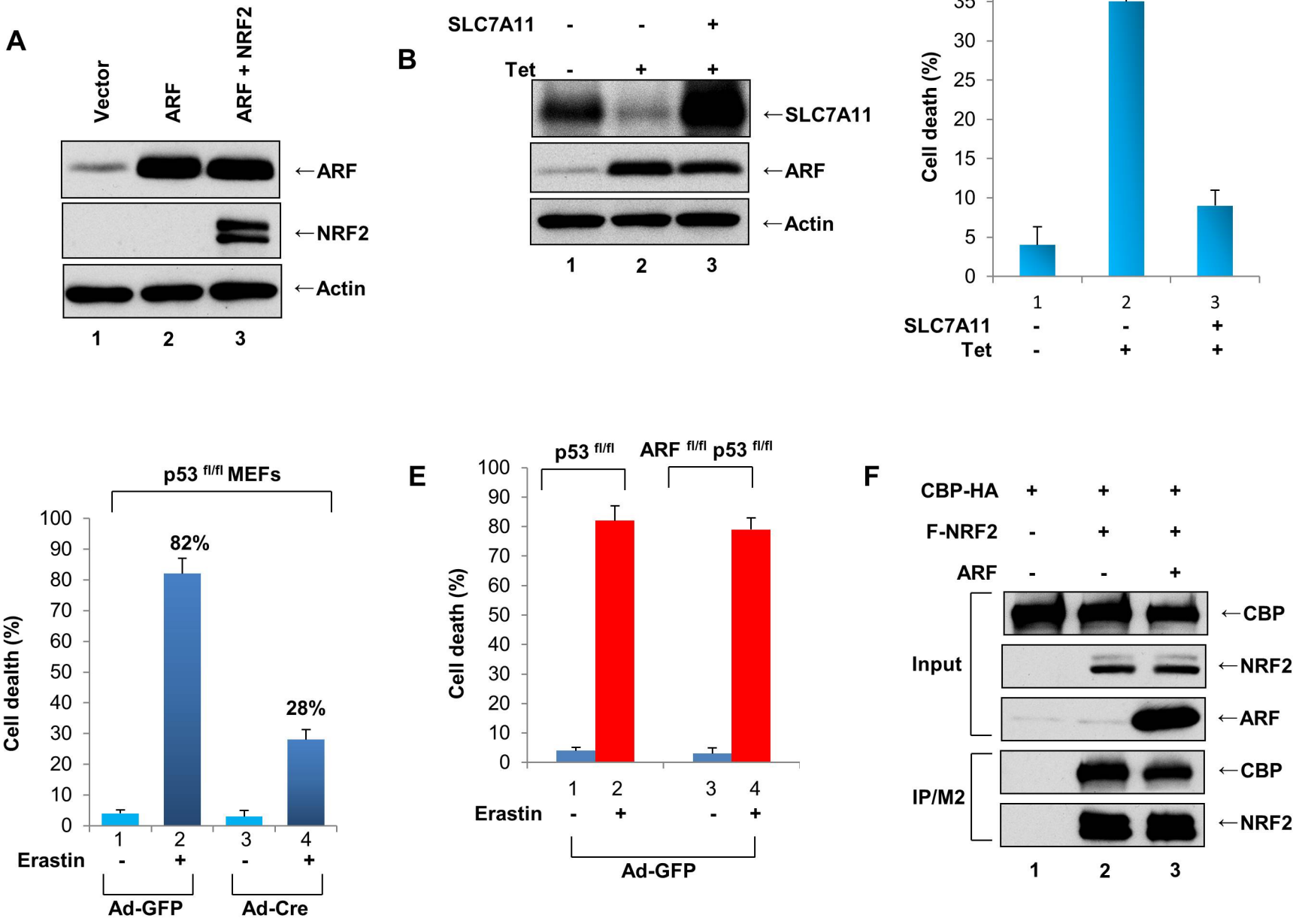
A
Vector
ARF
ARF + NRF2
←ARF
←NRF2
←Actin
1 2 3
B
SLC7A11 - - +
Tet - + +
←SLC7A11
←ARF
←Actin
1 2 3
C
Cell death (%)
40
35
30
25
20
15
10
5
0
1 2 3
SLC7A11 - - +
Tet - + +
D
p53 fl/fl MEFs
Cell death (%)
100
90
80
70
60
50
40
30
20
10
0
82%
28%
1 2 3 4
Erastin - + - +
Ad-GFP
Ad-Cre
E
p53 fl/fl
ARF fl/fl p53 fl/fl
Cell death (%)
100
90
80
70
60
50
40
30
20
10
0
1 2 3 4
Erastin - + - +
Ad-GFP
F
CBP-HA + + +
F-NRF2 - + +
ARF - - +
Input
←CBP
←NRF2
←ARF
IP/M2
←CBP
←NRF2
1 2 3

Figure S3. NRF2 expression abrogates ROS-induced cell death induced by ARF, related to Figure 3.

A. H1299 cells were transfected with an empty expression vector (lane 1), or expression vectors encoding ARF alone (lane 2), or ARF together with NRF2-V5 (lane 3), and extracts of these cells were immunoblotted with antibodies specific for V5 (to detect NRF2-V5), ARF and Actin.
B. H1299 ARF inducible cells were treated with doxycycline (lane 2, 3) versus control (lane 1), together transfected with an empty expression vector (lane 1, 2), or expression vectors encoding SLC7A11 (lane 3), and extracts of these cells were immunoblotted with antibodies specific for SLC7A11, ARF and Actin.
C. Quantification of ROS-induced cell death by TBH in ARF-inducible H1299 cells treated with or without doxycycline and/or overexpression of SLC7A11 as indicated (error bars, s.d. from three technical replicates).
D. Quantification of ferroptotic cell death in $p53^{fl/fl}$ MEFs treated with the Ad-Cre or the control Ad-GFP virus (error bars, s.d. from three technical replicates).
E. Quantification of ferroptotic cell death in $p53^{fl/fl}$ and $ARF^{fl/fl}$ /$p53^{fl/fl}$ MEFs treated with the control Ad-GFP virus with or without Erastin as indicated (error bars, s.d. from three technical replicates).
F. 293 cells were transfected with expression vectors encoding Flag-NRF2, CBP-HA, and/or ARF, as indicated. Cell lysates were immunoprecipitated with FLAG-M2 beads, and the fractionated proteins were blotted with antibodies specific for the Flag epitope (for Flag-NRF2), the HA epitope (for CBP-HA), or ARF.

Figure S4.

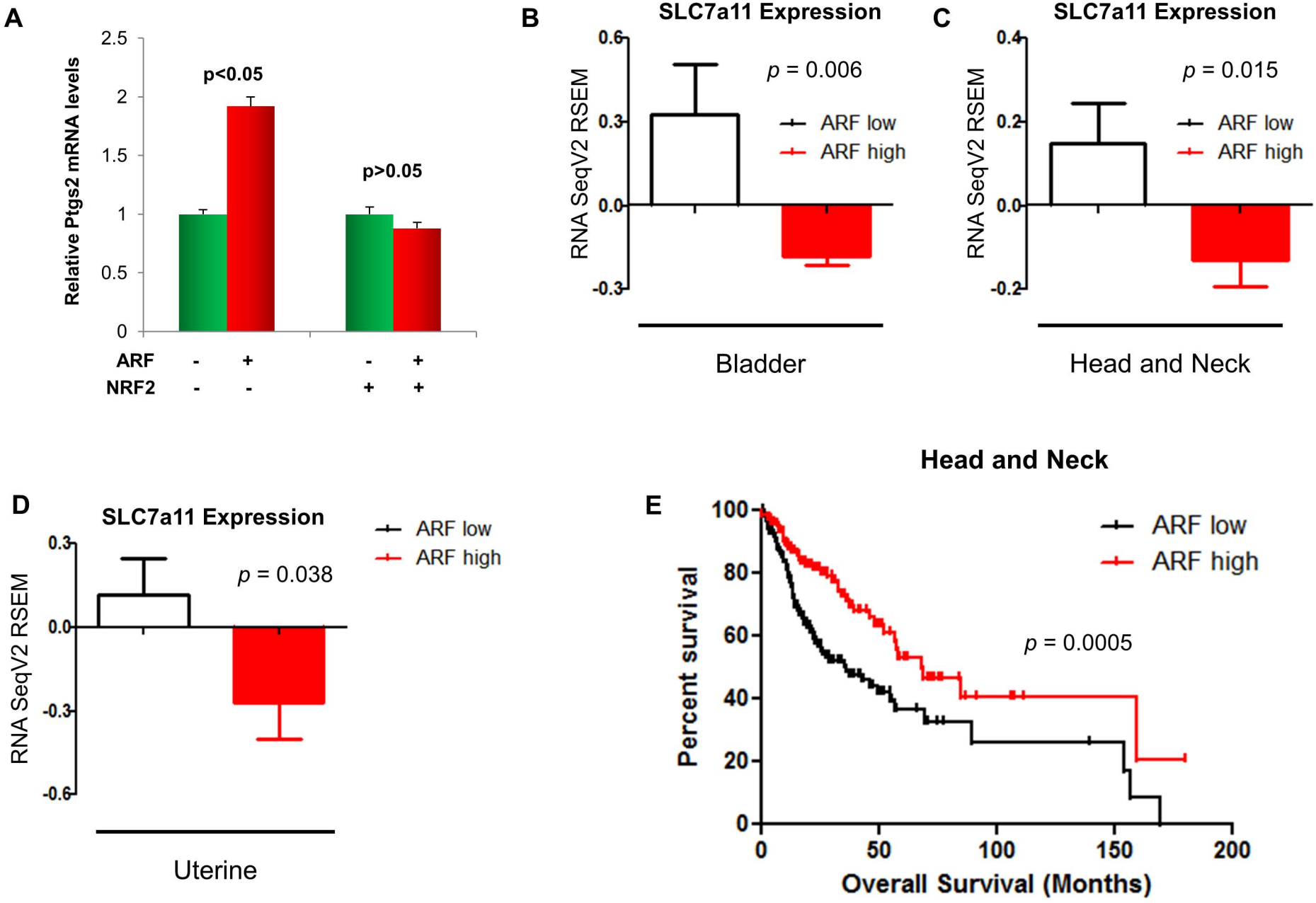
A
Relative Ptgs2 mRNA levels
2.5
2
1.5
1
0.5
0
p<0.05
p>0.05
ARF - + - +
NRF2 - - + +
B
SLC7a11 Expression
RNA SeqV2 RSEM
0.6
0.3
0.0
-0.3
p = 0.006
ARF low
ARF high
Bladder
C
SLC7a11 Expression
RNA SeqV2 RSEM
0.4
0.2
0.0
-0.2
p = 0.015
ARF low
ARF high
Head and Neck
D
SLC7a11 Expression
RNA SeqV2 RSEM
0.3
0.0
-0.3
-0.6
p = 0.038
ARF low
ARF high
Uterine
E
Head and Neck
Percent survival
100
80
60
40
20
0
0
50
100
150
200
Overall Survival (Months)
p = 0.0005
ARF low
ARF high

Figure S4. There is an inverse correlation between ARF expressions and levels of NRF2 in human tumor specimens, related to Figure 4.

A. qPCR analysis of Ptgs2 mRNA levels from Xenograft tumors in Figure 4D.

B-D. Gene expression from cBioPortal for Cancer Genomics data was analyzed from 3 datasets: Bladder Urothelial Carcinoma (n = 409; ARF low = 103, ARF high = 102), Head and Neck Squamous Cell Carcinoma (n = 522; ARF low = 131, ARF high = 131), and Uterine Corpus Endometrial Carcinoma (n = 178; ARF low = 45, ARF high = 45). Patient samples were stratified based on *CDKN2A* levels (ARF low-black; ARF high-red). Mean expression levels of *SLC7a11* were plotted and compared using a two-tailed students T-test ($p < 0.05$ denoted as significant).

E. Kaplan-Meier survival curve was generated for overall survival by stratifying patient samples with Head and Neck Squamous Cell Carcinoma from cBioportal (n = 530) based on *CDKN2A* (ARF) expression levels. The tumor patients from higher and lower quartiles for *CDKN2A* expression [ARF low (n = 130; black) and ARF high (n =130; red)] were extracted and analyzed by a log-rank test ($p=0.0005$).